The 19th Conference of mechanical Engineering Network of Thailand
19-21 October 2005, Phuket, Thailand

Analysis of Tin Powder Production Using a Pilot Gas Atomiser

C. Dungkratok[1], N. Srisukhumbowornchai[2], K. Fakpan[3], M. Morakotjinda[3],
N. Tosangthum[3], O. Coovattanachai[3], R. Krataitong[3], A. Daraphan[3],
B. Vetayanugul[3] and R. Tongsri[3]

[1] Department of Production Technology, Faculty of Engineering, King Mongkut's Institute of Technology North Bangkok, Bangkok 10800

[2] Materials Technology Division, School of Energy and materials, King Mongkut University of Technology Thonburi, 91 Pracha U-thit Rd., Bangmod, Tungkru, Bangkok 10140

[3] Powder Metallurgy Research and Development Unit (PM_RDU)
National Metal and Materials Technology Center (MTEC),
Thailand Science Park, 114 Paholyothin Rd. Klong Luang, Pathumthani, 12120
E-mail: kittichf@mtec.or.th

Abstract
Tin and tin alloy (Babbit metal) powders had been produced experimentally with varied processing factors such as nozzle design, melt flow, atomising gas pressure and melt superheat. Yield, particle size and microstructure of the powders were analysed. Particle size distribution of the powders was compared to a mean particle size calculated by using Lubanska's equation. It was found that the calculated mean particle size was closer to the experimental one when a constant *K* of Lubanska's equation was varied. Microstructures of tin and tin alloy powders indicated that solidification phenomena occurred via nucleation and growth.

Keywords: Powder production, gas atomiser, tin, tin alloy

1. Introduction

Powder production, using a gas atomisation process, has been being widely investigated and applied in industry [1], due to its advantages including high capacity, high flexibility for both elemental and prealloyed powder production and capability for rapidly solidified metal powder production. The rapidly solidified metal powders usually exhibit superior properties caused by fine microstructure, chemical homogeneity, extended solid solution and metastable phase formation. Therefore, metal parts produced from the rapidly solidified metal powders show superior mechanical properties.

In principle, when the metal melt is caused unstable by any forces it will be broken into forms of smaller pieces or droplets. Melt disintegration mechanism [2] in a gas atomisation process includes five steps as follows (Fig. 1);

(i) impingement of atomising gas on the melt causes unstable wavy melt stream
(ii) ligament formation occurs at the end of melt stream wave
(iii) ligament further discomposes into droplets (primary atomisation)
(iv) melt droplets are further disintegrated (secondary atomisation)
(v) satellite formation by crashing between melt droplets.

In a gas atomisation process, there are important factors controlling particle size and size distribution of the powders. The factors [3] include nozzle design, atomising gas flow rate, metal melt flow rate, type of metal melt and melt superheat. Investigation of processing parameters on powder particle size is very useful because information, correlation and prediction models are needed by powder production industry.

Investigation on atomisation of water and oil by Wigg [4] yielded an equation, which could be used for metal melt atomisation. The equation is as follows;

$$D_m = 20\delta^{0.1}\sigma^{0.2}\rho_g^{-0.3}\nu_m^{0.5}U_g^{-1.0}M^{0.1}[1+(M/A)]^{0.5} \quad (1)$$

where $U_g = (\gamma P_g / \rho_g)^{0.5}$

d_m = averaged size of metal powder particles δ
= diameter of melt feed tube
ρ_g = gas density
ν_m = kinematic viscosity of the melt
M = melt flow rate
A = atomising gas velocity
P_g = gas pressure.

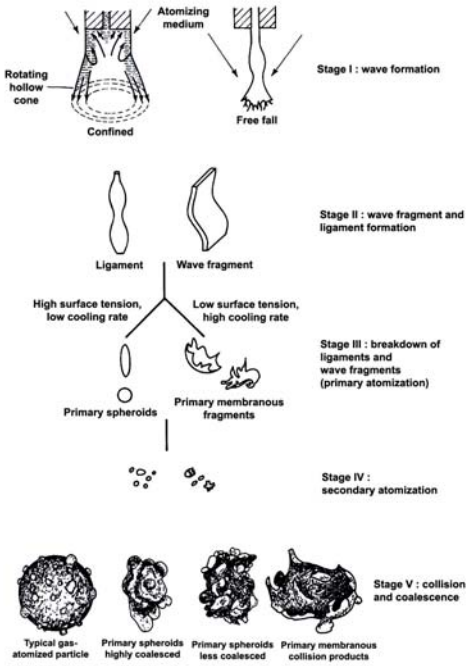

Figure 1. Gas atomisation mechanism.

One of the famous studies on processing parameter-powder particle size correlation was carried out by Lubanska [5]. Investigation on production of metal powders (iron, aluminium and tin) resulted in Wigg's equation modification. Lubanska's equation is as follows;

$$\frac{d_m}{\delta} = K\left[\frac{\nu_m}{\nu_g We}\left(1+\frac{M}{A}\right)\right]^{0.5} \qquad (2)$$

where $We = \dfrac{\rho_g \Delta U^2 \delta}{\sigma}$

K = constant

ν_g = kinematic viscosity of a gas

We = Weber number.

In this investigation, results obtained from tine and tin alloy (Babbitt) powder production have been analysed compared to the Lubanska's equation.

2. Materials and Methods

(2.1) Materials and equipment

Materials employed for this investigation were tin and tin alloy (Babbitt). Their chemical compositions, analysed by X-Ray fluorescence (XRF), is shown in Table 1. A gas atomiser used for metal powder production is shown in Fig. 2. Two types of nozzles, namely confined and free-fall nozzles (Fig. 3), were used. Effect of nozzle design was determined.

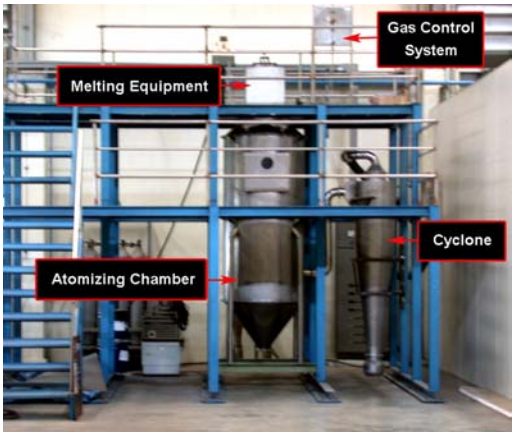

Figure 2. The pilot gas atomiser.

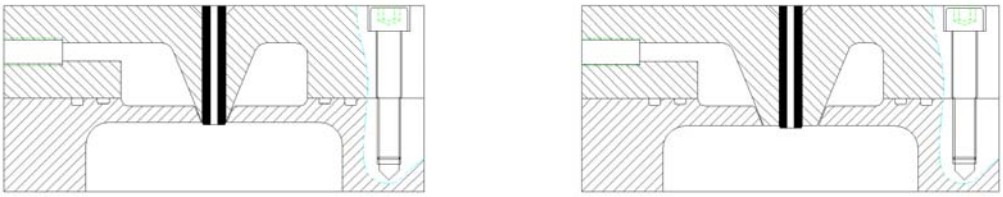

(a) (b)

Figure 3. Sketches of confined (a) and free-fall (b) nozzles.

Table 1 Chemical compositions of tin and Babbitt

Elements	Sn (%)	Sb (%)	Al (%)	P (%)	Cu (%)	Others (%)
Tin	99.6	-	0.0157	0.0158	0.274	0.0945
Babbitt	83.04	10.19	-	-	5.50	1.27

(2.2) Experimental procedure

Tin and Babbitt were melted in a furnace. Superheat temperature of both metal melts were 68 °C. The melt was released through a melt feed tube. When it emerged from the tube, it was crashed with high-velocity nitrogen gas. Impingement between gas and melt resulted in formation of flakes, ligaments and spherical powder particles. All the atomised products were sieved. The quantity of powders with particle size less than 180 μm was used for weight fraction calculation and powder particle characterisation. Experimental procedure is illustrated in Fig. 4.

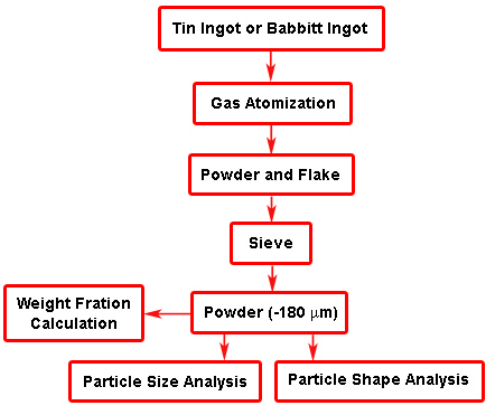

Figure 4. Experimental procedure.

3. Results and Discussion

(3.1) Powder particle size

Experimental values of tin and Babbitt powder particle sizes were obtained by using a powder particle size analyzer. Calculation of the powder particle sizes was carried out by using Lubanska's equation (Equation (2)). Materials property (Table 2) and nozzle constant (Table 3) were taken for calculating of the powder particle size. The constant K in Lubanska's equation was recommended to be in the range of 40-50. The gas flow rate (A) and melt flow rate (M) were calculated according to equations (3) and (4), respectively.

$$A = a\left(\frac{2}{k_T+1}\right)^{k_T+1/2(k_T-1)}\frac{P\sqrt{2g}}{\sqrt{RT}} \qquad (3)$$

where a = gas exit area

k_T = ratio between specific heat capacity of an atomising gas at a constant pressure and specific heat capacity of the atomising gas at a constant temperature (C_p/C_v)

g = gravitational acceleration

R = gas constant

T = gas temperature.

$$M = a_m\rho_m\left[2gh+\frac{2\Delta P}{\rho_m}\right]^{\frac{1}{2}} \qquad (4)$$

where a_m = melt exit area

ρ_m = melt density

h = height of melt in a crucible

ΔP = pressure difference between a crucible and an atomising chamber.

Plots of experimental and calculated values of powder particle size against gas pressure for confined and free-fall nozzles are presented in Figs. 5 and 6, respectively.

When the confined nozzle was employed the plots of experimental powder particle sizes of tin and Babbitt (Fig. 5) were similar to the plots between the calculated powder particle size against gas pressure. When the constant K = 40 was used, the plot of the calculated data moved closer to the plot of experimental ones. When the free-fall nozzle was employed, the plot of tin powder particle size was close to the plot of the calculated one, particularly when the constant K = 40 was used.

Figs. 5 and 6 indicate that the experimental powder particle sizes are smaller than the calculated ones. The powder particle size difference may be attributed to some reasons. The first is an error arisen from Weber number miscalculation. The second comes from the nature of the nozzle. A distance between the gas exit and impingement points is short so kinetic energy loss is low. This causes smaller powder particle formation. The last reason is attributed to the input data (materials property) for calculation. In this study, only property of tin was used. Tin property cannot represent Babbitt one.

(3.2) Powder morphology

The gas-atomised tin and Babbitt powders particles (Figs. 7 and 8) were typically spherical. Some particles showed evidences of satellite formation, which was caused by attachment of smaller solid powder particles onto larger melt droplets. The attachment was in turn attributed to turbulent flow of particles and gas in the atomising chamber.

(3.3) Powder microstructure

Cross section of a gas-atomised tin powder particle exhibited polycrystalline structure. In a coarse tin powder particle, there were some fine equi-axed grains (grain size < 20 μm) (Fig 9). Formation of this microstructural type is resulted from nucleation sites on the melt droplet surface. After nucleation, competitive growth of several nuclei occurs. When the solid/liquid interface of each nuclei meet, grain boundaries are formed.

Cross section of a gas-atomised Babbitt powder particle exhibited very fine precipitates of intermetallic Sn-Sb and Sn-Cu compounds homogeneously distributed in the matrix. The presence of intermetallic compounds causes difficulty for grain and grain boundary observation.

Table 2 Materials property

Materials property	Tin (300°C)	Nitrogen (25°C)
Density (kg/m^3)	6958.316	1.15
Molecular weight (kg/kmol)	-	28.013
Kinematic viscosity (m^2/s)	2.4458712x10^{-7}	1.55x10^{-5}
Surface tension (N/m)	0.53925	-
k_T (C_p/C_v)	-	1.41

Table 3 Nozzle constant

Parameter	Value
Gas exit area of the confined nozzle	1.79x10^{-5} m^2
Gas exit area of the free-fall nozzle	4.0x10^{-5} m^2
Melt exit area (3 mm)	7.07x10^{-6} m^2

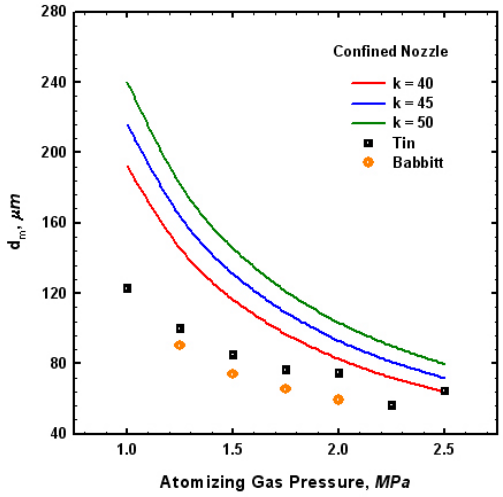

Figure 5. Plot of powder particle size against atomising gas pressure for the confined nozzle.

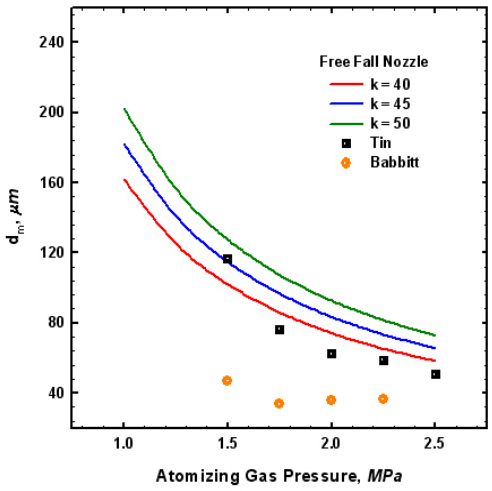

Figure 6. Plot of powder particle size against atomising gas pressure for the free-fall nozzle.

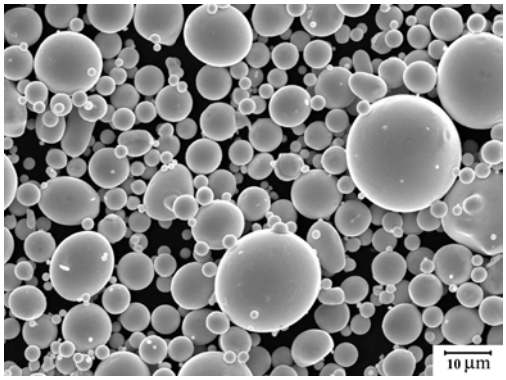

Figure 7. Morphology of gas-atomised tin powders.

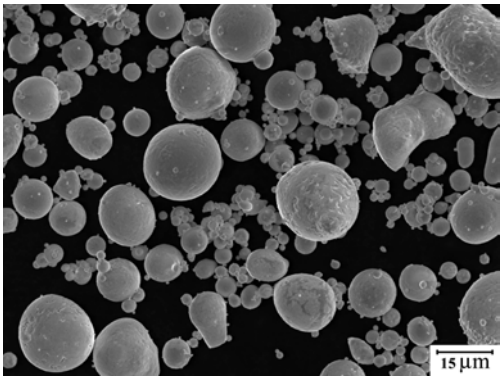

Figure 8. Morphology of gas-atomised Babbitt powders.

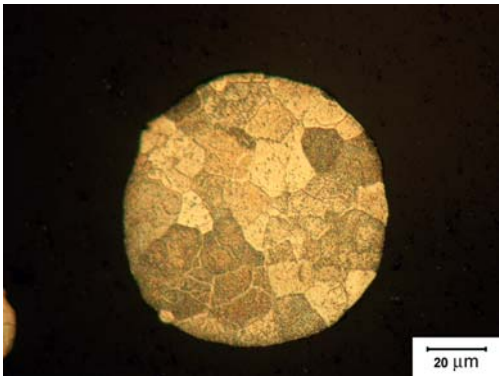

Figure 9. Microstructure of a gas-atomised tin powder particle.

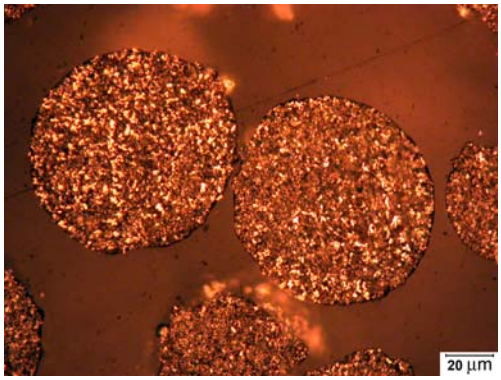

Figure 10. Microstructure of gas-atomised Babbitt powder particles.

Conclusions

(1) Lubanska's equation is useful for prediction of tin atomisation when the constant $K = 40$ is employed.
(2) Gas-atomised tin and Babbitt powders exhibited spherical shape.
(3) Microstructure of a gas-atomised tin powders clearly indicates that solidification occurs via nucleation and growth. In a gas-atomised Babbitt droplet, precipitation of intermetallic compounds occurs in addition to matrix solidification.

Acknowledgment

The authors would like to express their sincere gratitude to Metal and Materials technology Center (MTEC) for financial support for this investigation.

References

[1] J.J., Dunkly., "Gas atomization a review of the current state of the art ", Advances in Powder Metallurgy & Particulate Materials, 1999, pp. 55-66.
[2] E., Klar. and J.W., Fesko, "Gas and Water Atomization", ASM Handbook, Powder Metallurgy, Vol. 7, 1984, pp. 25-39.
[3] K. Fakpan, S. Morakotjinda, N. Tosangthum, O. Coovattanachai, R. Krataitong, S. Mata, A. Daraphan, B. Vetayanugul, N. Srisukhumbowornchai and R. Tongsri, "Production of Tin Powder by a Gas Atomisation", ***NSTDA Annual Conference 2005***, Pathum Thani, Thailand, March 28-30, 2005.
[4] L.D. Wigg, *J. Inst. Fuel*, Vol. .27, 1964, pp. 500.
[5] H. Lubanska, "Correlation of Spray Ring Data for Gas Atomization of Liquid Metals", *J. Met.*, Vol. 22, 1970, pp. 45-49.